

# Highway Propagation Modeling in VANETs and Its Impact on Performance Evaluation

Henrik Schumacher and Hugues Tchouankem

Institute of Communications Technology, Leibniz Universität Hannover, Germany

**Abstract**—Available simulation studies on communication performance of Vehicular Ad-Hoc Networks (VANETs) in highway scenarios are based on different propagation models, often without empirical validation. In this paper, we present the results of a 5.9 GHz vehicle-to-vehicle (V2V) highway measurement campaign using commercial off-the-shelf hardware to gain insights into adequate path loss modeling. As most established models significantly deviate from the empirical results, we propose a propagation model for V2V communication on highways which reflects conditions found in reality sufficiently well to be applicable for VANET simulation studies. Due to the propagation model's complex interdependencies with the CSMA-based medium access, interference and frame collisions in VANETs, we examine the impact of different propagation modeling approaches on the resulting communication performance for varying network loads based on a simulation study. The results reveal that both the applied path loss model and the severity of fading substantially influence the simulation results and hence should be modeled very carefully.

## I. INTRODUCTION

Vehicular Ad-Hoc Networks (VANETs) have the potential to significantly improve the level of safety, efficiency and comfort in next generation road traffic and hence have received considerable research attention in recent years. Safety applications in VANETs rely on 5.9 GHz vehicle-to-vehicle (V2V) communication based on IEEE 802.11 [1, 2]. As reproducible field tests involving large numbers of vehicles are hard to realize, performance evaluation in VANETs, especially with respect to scalability aspects, is predominantly based on simulation or analytical models. For this purpose, however, assumptions about the scenario-specific radio propagation in terms of path loss and signal fading have to be made, which are reflected by the applied propagation model.

Highway scenarios are of particular interest for safety applications based on V2V communication, and hence there are numerous valuable simulation studies on VANET performance in highway scenarios, which, however, use different propagation modeling approaches, mostly without empirical validation of the applied model. On the other hand, only few empirical studies on highway V2V propagation are available, e. g. [3–6]. Moreover, these studies present significant differences in their measurement methods as well as in their results. Motivated by these findings, we conduct a V2V highway measurement study, presented in section II, using test devices that meet the 802.11p [1] and ITS-G5 [2] specifications in order to gain insights into adequate path loss modeling in highway scenarios. Based on the results of our field tests, we propose a model for highway V2V propagation that reflects conditions

found in reality sufficiently well to be applicable for VANET simulation studies (see section III).

While empirical results from measurement studies on V2V propagation are generally based on interference-free conditions, scalability in VANET is limited by interference [7, 8]. For this reason, investigating the propagation model's impact on the communication performance under non-negligible co-channel interference is of particular interest, as this aspect directly affects the necessary level of accuracy in simulation-based performance evaluation. This motivates our simulation study presented in section IV, which examines the impact of different path loss models and severities of fading on the communication performance for varying network loads.

### A. Path Loss Modeling in VANETs

In the literature, several different path loss models are used for simulation studies on VANETs in highway scenarios. In the following, we shortly summarize these different models.

The *Free Space Path Loss Model* by Friis [9] presents the most basic model to quantify large-scale path loss as

$$PL(d) \text{ dB} = 10 \lg \left( \frac{16\pi^2 d^2}{G_t G_r \lambda^2} \right) \text{ dB}, \quad (1)$$

where  $d$  denotes the distance between transmitter and receiver,  $G_t, G_r$  their respective antenna gains and  $\lambda$  the wavelength corresponding to the carrier frequency  $f_c$ .

The *Log-Distance Path Loss Model* extends the Free Space Model by using a variable path loss coefficient  $\alpha$  that can be adapted according to the propagation environment, i. e.

$$PL(d) \text{ dB} = PL(d_0) \text{ dB} + \alpha 10 \lg \left( \frac{d}{d_0} \right) \text{ dB} \quad (2)$$

where  $d_0$  denotes a reference distance that the path loss is usually calculated for using the Free Space Model in Eq. 1. Simulation studies on highway V2V communication applying the Log-Distance Path Loss Model include [10] and [11] using  $\alpha = 2.15$  and  $\alpha = 2.31$ , respectively.

The *Two-Ray Ground Reflection Model* results from a superposition of the LOS signal and the transmitted signal's ground reflection involving the phase difference between both signal components. Sommer et al. [12] conduct V2V propagation measurements under completely unobstructed channel conditions and, based on their findings, recommend using the Two-Ray Ground Reflection Model for VANET simulation. In a highway scenario, however, channel conditions may deviate from this unobstructed environment.

A simplified version of the Two-Ray Ground Reflection Model, which we refer to as the *simplified Two-Ray Ground Model*, is applied very often in the context of VANET simulation studies, e. g. [7, 8, 13–15]. This model assumes that path loss corresponds to the Free Space Model for distances smaller or equal to the crossover distance  $d_c$ , but increases with the fourth power of  $d$  for greater distances, i. e.

$$PL(d) \text{ dB} = \begin{cases} 10 \lg \left( \frac{16\pi^2 d^2}{G_t G_r \lambda^2} \right) \text{ dB}, & d \leq d_c \\ 10 \lg \left( \frac{d^4}{G_t G_r h_t^2 h_r^2} \right) \text{ dB}, & d > d_c \end{cases} \quad (3)$$

where  $h_t$  and  $h_r$  are the transmitter and receiver antenna heights, respectively. The crossover distance is calculated by equating both terms, resulting in

$$d_c = \frac{4\pi h_t h_r}{\lambda}. \quad (4)$$

The *Dual-Slope Model* provides more flexibility by quantifying path loss as a piecewise linear function on a log-log scale as

$$PL(d) \text{ dB} = PL(d_0) \text{ dB} + \begin{cases} \alpha_1 10 \lg \left( \frac{d}{d_0} \right) \text{ dB}, & d \leq d_{bp} \\ \alpha_1 10 \lg \left( \frac{d_{bp}}{d_0} \right) \text{ dB} + \alpha_2 10 \lg \left( \frac{d}{d_{bp}} \right) \text{ dB}, & d > d_{bp} \end{cases} \quad (5)$$

where  $\alpha_1$  and  $\alpha_2$  denote the path loss coefficients that have to be determined empirically and  $d_{bp}$  the breakpoint distance that marks the transition between  $\alpha_1$  and  $\alpha_2$ . Based on extensive measurement studies on U.S. highways, Cheng et al. [6] and Stancil et al. [16] conclude that the Dual-Slope Model presents a good approximation of the empirical data if  $\alpha_1 = 2.0$ ,  $\alpha_2 = 4.0$  and the breakpoint distance

$$d_{bp} = \frac{4h_t h_r}{\lambda} \quad (6)$$

are used. It can be shown that this approximates the distance where the first Fresnel ellipsoid touches the ground, i. e. the path length difference between the LOS component and the ground reflection corresponds to a phase difference of  $\pi$  [17].

### B. Modeling Signal Fading in VANETs

Due to pronounced multipath propagation in VANETs, the received signal is subject to significant small-scale signal fading, which has to be considered in the context of propagation modeling. The most popular model used for this purpose is the Nakagami fading model, which is probably attributable to its great flexibility. Moreover, several empirical studies support the applicability of Nakagami fading for highway V2V communication, e. g. [3, 16, 18], so we decide to employ this model for our simulation study presented in section IV.

If Nakagami fading is applied, the received power  $P_r$  follows a Gamma distribution with the shape parameter  $m$  (also referred to as the fading parameter) and the scale parameter  $\Omega_p/m$ , resulting in the probability density function

$$p(P_r) = \frac{m}{\Omega_p \Gamma(m)} \left( \frac{m P_r}{\Omega_p} \right)^{m-1} e^{-m P_r / \Omega_p}, \quad (7)$$

where  $\Gamma(\cdot)$  denotes the Gamma function and  $\Omega_p$  the mean received power, which can be calculated using one of the path loss models presented above. The Nakagami model is able to reflect different severities of fading: For  $m = 1$ , the model corresponds to Rayleigh fading, for  $m > 1$ , Ricean fading with parameter  $K$  is closely approximated by  $m = (K + 1)^2 / (2K + 1)$ , and for  $m \rightarrow \infty$ , the received signal does not show any fading.

The remainder of this paper is organized as follows: Section II presents our highway V2V measurement campaign and compares its empirical results to different path loss models. In section III, we describe the Highway Propagation Model, which presents a good approximation of propagation conditions found in reality. The setup and results of our simulation study that quantifies the impact of propagation modeling on simulation-based performance evaluation are presented in section IV. Finally, we conclude our work in section V.

## II. MEASUREMENT STUDY ON HIGHWAY V2V PROPAGATION

Motivated by the variety of path loss models for propagation modeling in VANETs, we conduct an empirical measurement study in order to investigate the applicability of the different path loss models for simulation of VANET highway scenarios. This measurement study is based on 5.9 GHz V2V field tests involving two vehicles on a German three-lane highway.

### A. Measurement Equipment

In order to gather empirical data that can be used for the derivation and validation of propagation models for vehicular communication, we employ custom measurement devices which are based on commercial off-the-shelf hardware and can be used for 5.9 GHz field tests. These devices were also used for previous studies presented in [19].

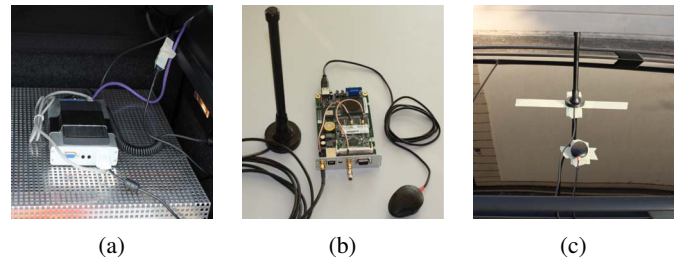


Figure 1: Communication device inside a vehicle's trunk (a), ALIX3D3 board with GPS receiver and magnetic mount antenna (b), antenna placement on vehicle roof (c).

Fig. 1 depicts the utilized hardware. The communication devices are based on a PC Engines ALIX3D3 mainboard running an Ubuntu Linux distribution. Each device is equipped with a Comex Mini PCI 802.11abg wireless card based on the Atheros AR5006X (AR5414) chipset. Navilock GPS receivers using the u-blox5 chipset allow logging the vehicle positions.

Furthermore, we equipped each vehicle with a vertically polarized magnetic mount antenna (Mobile Mark ECOM6-5500) placed in a central position on the vehicle's roof (see Fig. 1c).

On a metal ground plane, these antennas show an omnidirectional radiation pattern and a nominal antenna gain (including antenna cable attenuation) of 3.2 dBi at zero degrees elevation. Configuring the transmission power to 23 dBm and considering antenna gain as well as a system loss of approximately 3 dB caused by the connectors between interface card and external antenna, this results in an equivalent isotropically radiated power (EIRP) of 23.2 dBm.

As the measurement results are supposed to be applicable to prospective cooperative safety applications, the utilized wireless interfaces have to meet the IEEE 802.11p [1] or ITS-G5 [2] specifications. Hence, we use a modified driver based on ath5k and the Linux wireless subsystem. By this means, we are able to conduct tests on a 10 MHz channel centered at 5.9 GHz employing the Outside the Context of a Basic Service Set (OCB) mode [1, 2].

While the receiving wireless interface remains in monitor mode, passively listening to frames on the configured channel, a packet generator periodically creates messages on the transmitting node. At the receiver, a self-developed software tool utilizing the *libpcap* library is used to log the measured received signal strength indication (RSSI) values as well as the transmitter and receiver positions. RSSI values are extracted from radiotap headers and recorded for each successfully received frame. Moreover, a 32-bit sequence number allows derivation of the ratio of correctly received and transmitted frames, which we refer to as the packet delivery rate (PDR).

### B. Measurement Setup and Configuration

In order to conduct the field tests, each vehicle was equipped with a communication device including roof-mounted antenna and GPS receiver, as presented in subsection II-A. Several different vehicles were utilized, but in all cases, the antenna heights were approximately 1.5 m. During all measurements, one vehicle was configured as a transmitter, while another vehicle served as a receiver for the transmitted data.

Transmission power (EIRP)	23.2 dBm
Center carrier frequency	5.9 GHz
Channel bandwidth	10 MHz
Data rate	6 Mbps
Antenna height	1.5 m
Message generation rate	100 msg/s
MAC frame / message payload size	564 / 500 Bytes

Table I: Measurement system parameters.

Table I presents a summary of the measurement system parameters. The packet generator was configured to periodically generate messages with a generation rate of 100 msg/s and a net message size of 500 bytes. Including UDP, IP, LLC and MAC header (8/20/8/28 bytes), this results in a MAC frame size of 564 bytes. The frames are broadcasted in OCB mode using a data rate of 6 Mbps. This configuration represents periodic Cooperative Awareness Message (CAM) broadcasts.

Using this parameter set, a measurement study was conducted between exits 42 and 55 on the German highway Bundesautobahn 2, where the highway has three lanes per

direction. In total, the results we present in subsection II-C comprise measurement data collected on a covered distance of over 250 km. The transmitting and receiving vehicle moved in equal direction, but in varying sequence and on varying lanes with speeds between 90 and 135 km/h. We systematically varied the distance between both vehicles in order to gain insights into the resulting path loss as a function of distance.



Figure 2: Highway traffic during the measurements.

During all measurements, traffic density was occasionally moderate, but usually high and there was a significant portion of heavy vehicles (trucks, buses and RVs), which mainly moved on the right, partially on the center lane, and caused temporary non-line-of-sight (NLOS) situations (see Fig. 2). Furthermore, the course of the segment used for the field tests shows several hills, which, on the one hand, caused additional NLOS situations, but, on the other hand, can also temporarily increase the probability of a line-of-sight (LOS) connection.

### C. Measurements Results

In this section, we present the results acquired from the field tests and compare them to selected propagation models.

As already stated in previous work [19], a validation of the RSSI levels in a controlled lab environment reveals that, compared to the real received power, the RSSI values provided by *libpcap* contain a bias of approximately -3 dB for RSSI levels greater than -80 dBm and approximately -6 dB for those smaller than -80 dBm. We correct the RSSI results of the field tests accordingly to calculate the actual received power  $P_r$ .

In order to create insights from the field tests that can be used for the derivation and validation of propagation models for highway scenarios, we evaluate the received power as well as the packet delivery rate (PDR) based on the linear distance between transmitter and receiver. All measurements on the selected three-lane highway segment are evaluated aggregately, which allows the representation of a multitude of propagation effects in a statistically significant way. Fig. 3 depicts the results in terms of the received power  $P_r(d)$  for each frame, the received power's arithmetic mean  $\bar{P}_r(d)$  and the packet delivery rate  $PDR(d)$ . We compute  $\bar{P}_r(d)$  and  $PDR(d)$  for distance intervals of 10 m length and include 95 % confidence intervals (which are, however, very small) in the plots.

As expected, the results show severe signal fading, which can be recognized by a large variance of the measured received power  $P_r(d)$ . The results also reveal the approximate receiver sensitivity: While reliable frame reception is possible for  $P_r(d) \geq -93$  dBm, frames can only be decoded very infrequently for  $P_r(d) \leq -96$  dBm. Received power samples can only be collected for correctly received frames. Hence, the calculated arithmetic mean  $\bar{P}_r(d)$  reflects the real mean

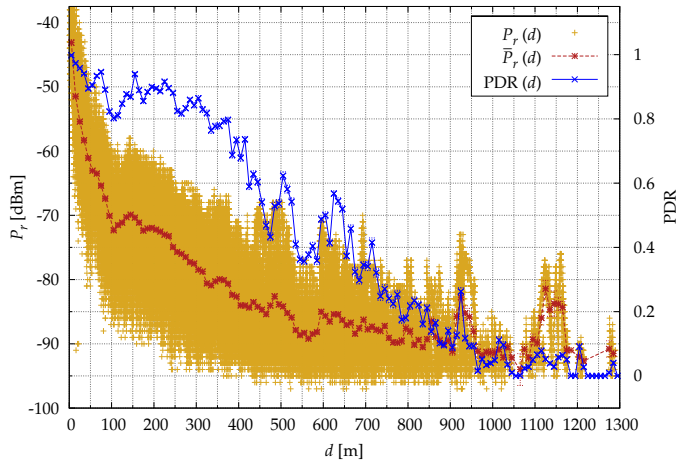


Figure 3: Measurement results from highway field tests - received power  $P_r(d)$  for each received frame, mean received power  $\bar{P}_r(d)$  and packet delivery rate  $PDR(d)$  as a function of distance  $d$  between transmitter and receiver.

received power sufficiently well for distances smaller than  $d \approx 350$  m, whereas for greater distances, which are associated with significantly lower PDRs, it significantly overestimates the real mean received power of all transmitted frames.

The PDR remains greater than 80% for  $d \leq 330$  m, but decreases quickly for  $d \geq 400$  m and only approximately 20% of the transmitted frames can be decoded for  $d = 800$  m. Less frequently, frames from greater distances can also be received successfully. Particularly for  $d \approx 930$  m and  $d \approx 1150$  m, we observe frames with a received power that is greater than expected. This can be attributed to situations where either the transmitter, the receiver or both are located on the top of a hill, allowing LOS communication even at great distances.

Fig. 4 compares the measured received power with the most popular path loss models used in VANET simulation studies, which are summarized in subsection I-A. The symbols  $d_{bp}$  and  $d_c$  denote the Dual-Slope Model's breakpoint distance and the simplified Two-Ray Ground Model's crossover distance, respectively.  $P_{r,th} = -91$  dBm denotes the receiver sensitivity that we assume for the simulation study presented in section IV, which is greater than the sensitivity that emerges from the measurement results, as we want to avoid modeling a best-case configuration. In addition to the aforementioned models from the literature, we use a modified version of the Dual-Slope Model with path loss coefficients  $\alpha_1 = 2.1$  and  $\alpha_2 = 3.4$ , as this presents the best agreement with the empirical data for  $d \leq 350$  m, the relevant area for curve fitting. The Dual-Slope Model proposed by Cheng, Stancil et al. [6, 16] using  $\alpha_1 = 2.0$ ,  $\alpha_2 = 4.0$  performs slightly worse, which may be attributable to differing propagation conditions in both measurement studies. For example, Cheng et al. report only moderate traffic during their highway measurements [6].

By contrast, the Free Space Model significantly underestimates path loss, particularly for larger distances, and hence significantly overestimates the achievable communication range. Interestingly, these characteristics also apply to

the simplified Two-Ray Ground Model, which is probably the most commonly employed path loss model in simulation tools as well as in existing VANET simulation studies investigating highway scenarios, e.g. [7, 8, 13–15]. This insight can mainly be attributed to the simplified Two-Ray Ground Model's crossover distance  $d_c$ , which is too large compared to propagation conditions found in highway field tests.

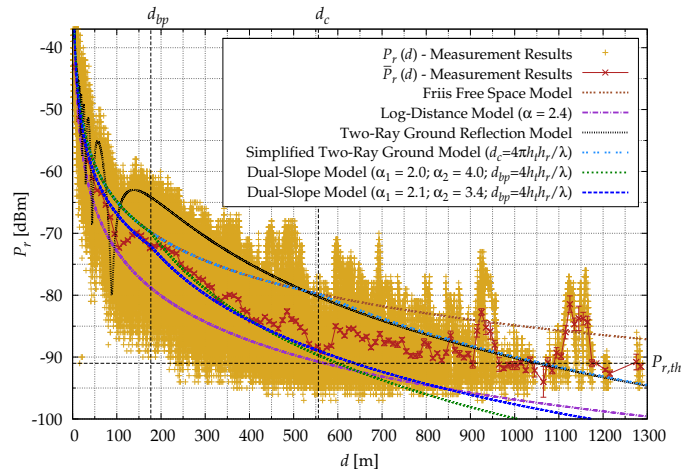


Figure 4: Comparison of received power  $P_r(d)$  and mean received power  $\bar{P}_r(d)$  acquired from field tests with results of different path loss models as a function of distance  $d$  between transmitter and receiver.

Concerning this matter, the results agree with Sommer et al. [12], who point out that the simplified Two-Ray Ground Model considerably underestimates path loss, and recommend using the Two-Ray Ground Reflection Model for VANET simulation studies instead, which applies a superposition of the LOS signal and the ground reflection. However, Fig. 4 reveals that this model does not reflect the propagation conditions found during the highway field tests sufficiently well, either. Considering the fairly high traffic density, this is probably caused by vehicles obstructing the LOS path or the ground reflection, which disagrees with the model's assumptions.

The Log-Distance Model using  $\alpha = 2.4$  presents an acceptable path loss estimation for larger distances and a good approximation of the achievable communication range, however, it significantly underestimates received power for small distances, which may cause an underestimation of interference and frame collisions in the context of simulation studies.

### III. HIGHWAY PROPAGATION MODEL

In the following, we present the Highway Propagation Model, which is designed to reflect radio propagation on three-lane highways in a satisfactory manner for simulation-based performance evaluation in VANETs and hence constitutes the basis of our simulation studies.

As a result from the field tests presented in section II, it can be concluded that the Dual-Slope Model satisfactorily reflects the path loss experienced in the highway scenario. However, the empirical results in Fig. 3 also confirm the presence of

severe fading, which has to be considered by the propagation model. Based on their results from measurement studies in a suburban environment, Cheng et al. [18] and Stancil et al. [16] conclude that the Nakagami model presents a good approximation of the signal fading. Furthermore, the authors show that the severity of fading significantly increases with distance, from Ricean fading ( $m > 1$ ) for small distances to pre-Rayleigh fading ( $m < 1$ ) for large distances. This behavior can be attributed to the decreasing probability of a dominant signal component with increasing distance.

Motivated by these findings, we decide to use the Nakagami model to incorporate the effects of signal fading into the Highway Propagation Model. Moreover, the model takes into account the distance dependence of the fading severity by describing the fading parameter  $m$  as a function of the distance  $d$  in meters,

$$m(d) = 2.7 \cdot e^{-0.01(d-1.0)} + 1.0 \quad , \quad (8)$$

resulting in moderate Ricean fading for small distances, as  $m(1.0 \text{ m}) = 3.7$ , while  $m$  asymptotically approaches Rayleigh fading for large distances, since  $\lim_{d \rightarrow \infty} m = 1.0$ . As dominant signal components are more likely to occur in highway scenarios than in suburban scenarios studied in [16, 18], which involve corners and turns, we assume Rayleigh instead of pre-Rayleigh fading for large distances. Table II summarizes the parameters of the Highway Propagation Model, which we use for the simulation study presented in the next section.

Parameter	Value	Parameter	Value
Path loss model	Dual-Slope (Eq. 5)	$f_c$	5.9 GHz
$G_t, G_r$	1.0	$h_t, h_r$	1.5 m
$d_0$	1.0 m	$PL(d_0)$	47.86 dB (Eq. 1)
$\alpha_1, \alpha_2$	2.1, 3.4	$d_{bp}$	177 m (Eq. 6)
Fading model	Nakagami-m	$m(d)$	see Eq. 8

Table II: Parameters of the Highway Propagation Model.

The Highway Propagation Model is based on an aggregate evaluation of the empirical data. For future work, an evaluation that distinguishes LOS and NLOS situations, which can particularly be caused by obstructing vehicles in highway scenarios, is envisaged to allow incorporating the channel coherence time into the propagation model. This, however, implies a significant increase of the simulation model's computational complexity, as it involves solving the geometric intersection problem to determine obstructing vehicles [20], which could present a challenge in the context of scalability studies.

#### IV. IMPACT OF PROPAGATION MODELS ON PERFORMANCE EVALUATION

The measurement study on highway propagation presented in section II and a comparison of its results with well-known path loss models reveal significant differences in the resulting received power. These differences imply complex interdependencies with the CSMA-based medium access, interference and frame collisions in VANETs. In the context of investigating scalability issues, the propagation model's impact on the

communication performance under non-negligible co-channel interference is of particular interest, as this aspect directly affects the necessary level of accuracy in simulation-based performance evaluation. To quantify this impact, we conduct a simulation study that examines the effects of selected propagation models and present its results in this section.

#### A. Simulation Setup

Our simulation environment relies on the well-known simulation tools SUMO, which provides road traffic simulation, and OMNeT++, which provides the basis for our network simulation. We extended the INETMANET framework for OMNeT++ by adding a model of the ITS protocol stack, particularly focusing on ITS-G5 and its medium access control. For this purpose, the implemented simulation model includes a detailed representation of co-channel interference and resulting frame collisions, including physical layer capture (PLC). Furthermore, the OCB mode is used for single-hop broadcast transmission of CAMs, which are periodically generated by each vehicle. In contrast to the IEEE 802.11 standard, we disable the post-backoff mechanism, i. e. stations have to perform the backoff procedure prior to each frame transmission. The path loss models summarized in section I as well as several fading and shadowing models including the Nakagami fading model are also implemented within the simulation model based on OMNeT++.

Parameter	Value	Parameter	Value
$P_t$	23 dBm	$f_c$	5.9 GHz
$G_t, G_r$	1.0	$h_t, h_r$	1.5 m
$f_g$	10 msgs/s	$CW$	15
Message size	400 Bytes	MAC frame size	480 Bytes
$R_b$	6 Mbps	$N$	-100 dBm
$SIR_{th}$	9 dB	$P_{r,th}$	-91 dBm
$P_{r,cs}$	-93 dBm	Fading model	Nakagami-m
$m(d)$	see Eq. 8		

Table III: Simulation parameters.

Table III summarizes the simulation parameters that all results presented in this section have in common, where  $P_t$  denotes the transmission power,  $f_c$  the carrier frequency,  $f_g$  the message generation rate,  $CW$  the contention window size, which is fixed as we only consider broadcast transmissions in this study,  $R_b$  the data rate used for transmission, and  $N$  the noise floor, respectively. The model assumes that a frame can be successfully decoded by the receiver if the Signal-to-Interference-and-Noise Ratio (SINR) during frame reception is greater or equal to  $SIR_{th}$ . The corresponding received power threshold allowing successful frame reception in absence of interference is referred to as the receiver sensitivity  $P_{r,th}$ , and  $P_{r,cs}$  denotes the carrier sense threshold. In addition to the insights from the field tests (see Fig. 3), we verified  $P_{r,th}$  in lab tests utilizing the same test devices and adjustable attenuators. The receiver sensitivity used in simulations contains additional offsets of approximately 3 dB and 6 dB compared to the sensitivity that emerges from the field tests and lab tests, respectively, to avoid modeling a best-case configuration.

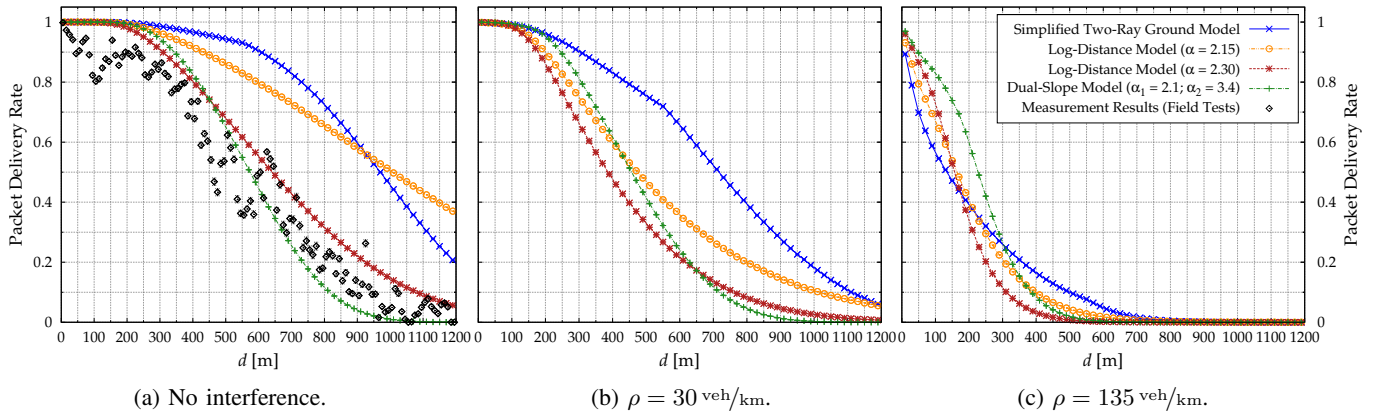


Figure 5: Comparison of PDRs acquired from field tests and simulation results using distance-dependent Nakagami fading according to Eq. 8 and different path loss models for interference-free conditions (a), low (b) and high network load (c).

Using SUMO's Traffic Control Interface (TraCI), the traffic simulator provides OMNeT++ with each vehicle's mobility data. In agreement with the field test scenario, the simulation scenario created in SUMO consists of a highway section with three lanes per direction. Although the total length of the section is 10 km, only a segment of 2 km length located at the scenario's center is used for statistical evaluation in order to eliminate boundary effects. Vehicles enter the scenario following a Poisson process, and their average speed is 120 km/h. We examine different values of the average traffic density  $\rho$ , which quantifies the aggregated number of vehicles per km for all highway lanes and both directions, resulting in different network loads. All investigated traffic configurations reflect free-flow traffic. The lowest traffic density used,  $\rho = 30 \text{ veh/km}$ , corresponds to sparse traffic with an average distance of 200 m between subsequent vehicles on the same lane, the highest density,  $\rho = 135 \text{ veh/km}$ , represents heavy traffic close to the highway section's capacity and an average distance of 44 m.

### B. Simulation Results

In this subsection, we present the results of our simulation study, which consist of two parts. While the first part investigates the impact of the path loss model using identical fading models, the second part examines the impact of the severity of fading on the resulting VANET communication performance.

1) *Impact of Path Loss Modeling*: For different interference levels, Fig. 5 illustrates the impact of the adopted path loss model on the PDR based on the parameters summarized in Table III. All path loss models are combined with Nakagami fading of distance-dependent severity, i. e. the results for the Dual-Slope model using  $\alpha_1 = 2.1$  and  $\alpha_2 = 3.4$  correspond to the Highway Propagation Model presented in section III.

Fig. 5a compares the interference-free PDR resulting from simulation configurations using different path loss models with the field test results, which also present interference-free conditions. The Dual-Slope Model (see Eq. 5) closely agrees with the empirical results, which supports the applicability of the Highway Propagation Model. While the Log-Distance Model (see Eq. 2) using  $\alpha = 2.3$  presents a good approximation of

the PDR in absence of interference, both the simplified Two-Ray Ground Model (see Eq. 3) and the Log-Distance Model using  $\alpha = 2.15$  significantly overestimate the interference-free PDR, and thus the achievable communication range.

For non-negligible network loads, however, periodic broadcast communication performance in VANETs is considerably influenced by interference. Hence, we are particularly interested in gaining insights into the complex interdependencies between propagation modeling, interference and communication performance. For this purpose, Fig. 5b and 5c present the PDR acquired from simulations considering interference for scarce ( $\rho = 30 \text{ veh/km}$ ) and dense ( $\rho = 135 \text{ veh/km}$ ) road traffic, implicating low and high network load, respectively.

The results clearly illustrate the substantial impact of the employed path loss model on the PDR and hence on the communication performance in VANETs. In this context, network conditions limited by path loss and those limited by interference can be distinguished. For path loss limited conditions, which can be assumed for all distances in the case of  $\rho = 30 \text{ veh/km}$  in Fig. 5b, path loss models that generally overestimate the received power, as the simplified Two-Ray Ground Model, also overestimate the PDR for all distances.

Higher network loads result in an increasing impact of interference. For  $\rho = 135 \text{ veh/km}$  in Fig. 5c, interference-limited conditions can at least be assumed for small distances. A general overestimation of the received power, as induced by the simplified Two-Ray Ground Model, also results in an overestimation of interference, which causes an underestimation of the PDR for low distances. With increasing distance, the impact of performance limitation caused by path loss gains importance and for large distances, a greater estimated received power also entails a greater PDR in this configuration.

Compared with the empirically validated Highway Propagation Model, the simplified Two-Ray Ground Model shows an absolute error of up to 41 % for low ( $d = 630 \text{ m}$ , see Fig. 5b) and 27 % for high network load ( $d = 130 \text{ m}$ , see Fig. 5c). Both configurations using the Log-Distance Model also show significant deviations, especially for high network load. The Log-Distance Model using  $\alpha = 2.3$ , which provides acceptable results in absence of interference, significantly underestimates

the PDR for  $\rho = 135 \text{ veh/km}$  in Fig. 5c, as it underestimates the received power for small distances. Additional simulations involving  $m = 3$  and  $m = 5$  reveal that these significant differences also occur for lower severities of fading.

2) *Impact of Fading Severity*: Inter-vehicular radio propagation is subject to severe signal fading, as the results in Fig. 3 and previous studies by other research groups show [5, 6, 18]. For suburban V2V communication, Cheng et al. [18] and Stancil et al. [16] found that fading can be adequately represented by a Nakagami model with a distance-dependent severity of fading which starts with Ricean fading for small distances, but quickly approaches and even exceeds Rayleigh fading for larger distances. For highway scenarios, our field test results indicate that a distance-dependent fading parameter  $m$  represents a good approximation of real propagation conditions if  $m$  reflects Ricean fading of moderate severity for small distances and quickly approaches, but does not exceed Rayleigh fading ( $m = 1$ ) for larger distances (see Eq. 8 and Fig. 5a).

While these measurement results are based on interference-free conditions, we are interested in the fading severity's impact on simulation-based performance evaluation under non-negligible co-channel interference. Hence, our simulation study investigates the impact of different fading severities based on the same path loss model. We use the Dual-Slope Path Loss Model ( $\alpha_1 = 2.1, \alpha_2 = 3.4$ ) for this purpose, which shows the best agreement with our field test results.

The simulation results in Fig. 6 illustrate the impact of the fading severity on the PDR for low ( $\rho = 30 \text{ veh/km}$ , see Fig. 6a) and high ( $\rho = 135 \text{ veh/km}$ , see Fig. 6b) network load. If no fading model is applied, the Dual-Slope Path Loss Model using  $\alpha_1 = 2.1$  and  $\alpha_2 = 3.4$  results in a deterministic communication range of  $d_{cr,det} = 638 \text{ m}$  under interference-free conditions, which are not depicted here.

For low network load (see Fig. 6a), the PDR already decreases in smaller distances due to frame collisions. Nevertheless, the results are qualitatively comparable to the interference-free case, i.e. more severe fading results in a smoother PDR curve, indicating a lower probability of successful frame reception for distances  $d < d_{cr,det}$ , but a higher probability for  $d > d_{cr,det}$ . Moreover, if no fading is applied, the robust range against hidden stations [7], which is  $d_{robHS} = 257.5 \text{ m}$  for this configuration, can be clearly identified in Fig. 6a. The fact that the PDR significantly decreases for  $d > d_{robHS}$  reveals a dominant impact of hidden station collisions on the communication performance.

With increasing network load, however, the impact of the fading severity is reversed. Fig. 6b reveals that for  $\rho = 135 \text{ veh/km}$ , which represents a severely congested network configuration, an increasing severity of fading results in a significant PDR improvement for small and medium distances. This result implies that for high network load, fading considerably increases the reliability of communication in the safety-relevant vicinity of a vehicle. The observed effect can be explained in conjunction with physical layer capture (PLC), which is part of the simulation model as well as real IEEE 802.11 receivers. Using PLC, a frame can be correctly

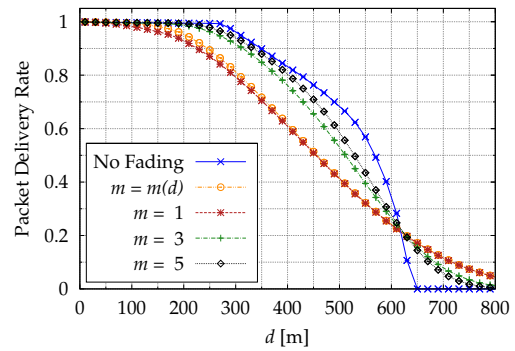
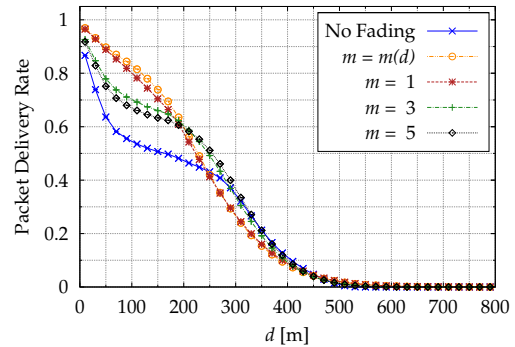
(a)  $\rho = 30 \text{ veh/km}$ .(b)  $\rho = 135 \text{ veh/km}$ .

Figure 6: Impact of fading severity on the PDR for Dual-Slope path loss combined with Nakagami fading for low (a) and high (b) traffic density.

received despite interference by another frame if the SINR threshold is exceeded, regardless of the chronological order of both frame arrivals. With an increasing severity of fading, the probability of large differences between the received powers of both frames increases, which results in an increased probability of successful frame reception.

## V. CONCLUSION

Motivated by the differences among propagation models applied in simulation studies on VANET performance, we conducted a V2V highway measurement study in order to gain insights into adequate path loss modeling in highway scenarios. The results indicate that most established VANET path loss models substantially deviate from conditions found in reality. We proposed a propagation model for V2V communication on highways using the Dual-Slope Path Loss Model and Nakagami fading with distance-dependent severity, which reflects conditions found in reality sufficiently well to be applicable for VANET simulation studies.

Furthermore, as the propagation model's impact on communication performance under non-negligible co-channel interference is of major interest in the context of scalability studies in VANETs, we examined the consequences of applying different path loss models and severities of fading using a simulation study. The results reveal that both for low and high network load, the PDR resulting from established path loss models (simplified Two-Ray Ground, Log-Distance) substantially de-

viates from the empirically validated Highway Propagation Model using Dual-Slope Path Loss, exhibiting absolute errors of up to 41 % and 27 %, respectively. Furthermore, we showed that the severity of fading significantly influences the resulting performance. For high network loads, severe fading can even improve the reliability of communication within the safety-relevant vicinity of a vehicle due to physical layer capture.

In summary, it can be stated that accurate propagation modeling is an important issue in simulation-based VANET performance evaluation, as it directly affects the accuracy of simulation results. Empirical validation of propagation models as well as a closer collaboration between the channel modeling and networking communities may contribute to resolve existing uncertainties in this context.

#### ACKNOWLEDGMENT

The authors are grateful to the Ministry of Science and Culture of Lower Saxony for funding our work within the Connected Cars in a Connected World (C3World) project. Furthermore, we thank Tetiana Zinchenko and Jörg Nuckelt for their valuable support during the measurements.

#### REFERENCES

- [1] *Wireless LAN Medium Access Control (MAC) and Physical Layer (PHY) Specifications - Amendment 6: Wireless Access in Vehicular Environments*. IEEE 802.11p-2010.
- [2] *Intelligent Transport Systems (ITS); European Profile Standard for the Physical and Medium Access Control Layer of Intelligent Transport Systems Operating in the 5 GHz Frequency Band*. ETSI ES 202 663 V1.1.0, 2010.
- [3] V. Taliwal, D. Jiang, H. Mangold, C. Chen, and R. Sengupta, "Empirical Determination of Channel Characteristics for DSRC Vehicle-to-Vehicle Communication," in *Proc. of the 1st ACM Int. Workshop on Vehicular Ad Hoc Networks (VANET'04)*. New York, NY, USA: ACM, 2004.
- [4] A. Paier, J. Karedal, N. Czink, H. Hofstetter, C. Dumard, T. Zemen, F. Tufvesson, A. F. Molisch, and C. F. Mecklenbräuker, "Car-to-Car Radio Channel Measurements at 5 GHz: Pathloss, Power-Delay Profile, and Delay-Doppler Spectrum," in *4th Int. Symp. on Wireless Communication Systems*. IEEE, Oct. 2007, pp. 224–228.
- [5] J. Kunisch and J. Pamp, "Wideband Car-to-Car Radio Channel Measurements and Model at 5.9 GHz," in *2008 IEEE 68th Vehicular Technology Conf.* IEEE, 2008.
- [6] L. Cheng, B. E. Henty, F. Bai, and D. D. Stancil, "Highway and Rural Propagation Channel Modeling for Vehicle-to-Vehicle Communications at 5.9 GHz," in *2008 IEEE Antennas and Propagation Society Int. Symp.* IEEE, Jul. 2008.
- [7] M. Torrent Moreno, *Inter-Vehicle Communications: Achieving Safety in a Distributed Wireless Environment*. Ph.D. dissertation, Univ.-Verl. Karlsruhe, 2007.
- [8] F. Schmidt-Eisenlohr, *Interference in Vehicle-to-Vehicle Communication Networks*. Ph.D. dissertation, Univ.-Verl. Karlsruhe, 2010.
- [9] H. T. Friis, "A Note on a Simple Transmission Formula," *Proc. of the IRE*, vol. 34, no. 5, 1946.
- [10] T. ElBatt, S. K. Goel, G. Holland, H. Krishnan, and J. Parikh, "Cooperative Collision Warning Using Dedicated Short Range Wireless Communications," in *Proc. of the 3rd ACM Int. Workshop on Vehicular Ad Hoc Networks (VANET'06)*. New York, NY, USA: ACM, 2006.
- [11] C.-L. Huang, Y. P. Fallah, R. Sengupta, and H. Krishnan, "Information Dissemination Control for Cooperative Active Safety Applications in Vehicular Ad-Hoc Networks," in *Proc. of the IEEE Global Telecommunications Conf. 2009 (IEEE GLOBECOM 2009)*. IEEE, Nov. 2009.
- [12] C. Sommer and F. Dressler, "Using the Right Two-Ray Model? A Measurement based Evaluation of PHY Models in VANETs," in *17th ACM Int. Conf. on Mobile Computing and Networking (MobiCom 2011), Poster Session*. Las Vegas, NV: ACM, Sep. 2011.
- [13] Q. Xu, T. Mak, J. Ko, and R. Sengupta, "Vehicle-to-Vehicle Safety Messaging in DSRC," in *Proc. of the 1st ACM Int. Workshop on Vehicular Ad Hoc Networks (VANET'04)*. New York, NY, USA: ACM, 2004.
- [14] J. Mittag, F. Schmidt-Eisenlohr, M. Killat, J. Härrig, and H. Hartenstein, "Analysis and Design of Effective and Low-Overhead Transmission Power Control for VANETs," in *Proc. of the 5th ACM Int. Workshop on Vehicular Inter-Networking (VANET'08)*. New York, NY, USA: ACM, 2008.
- [15] N. An, J. Mittag, F. Schmidt-Eisenlohr, and M. Torrent Moreno, "Accurate Knowledge of Radio Channel and Network Conditions - When Does it Matter?" in *8th Annu. Conference on Wireless On-Demand Network Systems and Services (WONS)*, Bardonecchia, Italy, 2011.
- [16] D. D. Stancil, F. Bai, and L. Cheng, "Communication Systems for Car-2-X Networks," in *Vehicular Networking: Automotive Applications and Beyond*, M. Emmelmann, B. Bochow, and C. C. Kellum, Eds. John Wiley & Sons, Ltd, Chichester, UK, 2010.
- [17] A. F. Molisch, *Wireless Communications*, 2nd ed. Piscataway, NJ: John Wiley & Sons, Ltd, 2010.
- [18] L. Cheng, B. Henty, D. Stancil, F. Bai, and P. Mudalige, "Mobile Vehicle-to-Vehicle Narrow-Band Channel Measurement and Characterization of the 5.9 GHz Dedicated Short Range Communication (DSRC) Frequency Band," *IEEE Journal on Selected Areas in Communications*, vol. 25, no. 8, Oct. 2007.
- [19] H. Schumacher, H. Tchouankem, J. Nuckelt, T. Kürner, T. Zinchenko, A. Leschke, and L. Wolf, "Vehicle-to-Vehicle IEEE 802.11p Performance Measurements at Urban Intersections," in *2012 IEEE Int. Conf. on Communications (ICC)*, Ottawa, Canada, 2012, pp. 7131–7135.
- [20] M. Boban, T. T. V. Vinhoza, M. Ferreira, J. Barros, and O. K. Tonguz, "Impact of Vehicles as Obstacles in Vehicular Ad Hoc Networks," *IEEE Journal on Selected Areas in Communications*, vol. 29, no. 1, pp. 15–28, Jan. 2011.